The International Archives of the Photogrammetry, Remote Sensing and Spatial Information Sciences, Volume XLVIII-M-9-2025
30th CIPA Symposium "Heritage Conservation from Bits:
From Digital Documentation to Data-driven Heritage Conservation", 25–29 August 2025, Seoul, Republic of Korea

Analysis of the Photogrammetry Use of Videos from 360-Degree Multicameras in Heritage-Related Scenes: Case of the Necropolis of Qubbet El-Hawa (Aswan, Egypt)

José Miguel Gómez-López [1], José Luis Pérez-García [1], Antonio Tomás Mozas-Calvache [1], Diego Vico-García [1]

[1] Dept. Ing. Cartográfica, Geodésica y Fotogrametría, University of Jaén, 23071 Jaén, Spain - (jglopez, jlperez, antmozas, dvico)@ujaen.es

Keywords: 360-Degree Camera, Videogrammetry, TLS, Close-Range Photogrammetry.

Abstract

This paper investigates the photogrammetric potential of 360-degree multi-cameras in complex heritage scenes, applied both indoors and outdoors at the Necropolis of Qubbet el-Hawa (Aswan, Egypt). While 360-degree cameras are increasingly used for heritage documentation due to their enhanced Field of View (FoV) and facilitated data acquisition, they still present limitations in geometric accuracy compared to techniques like Terrestrial Laser Scanning (TLS) or Close-Range Photogrammetry (CRP). Furthermore, indoor environments introduce additional challenges, particularly concerning illumination. These advantages and disadvantages are more pronounced when working with videos instead of still images: video acquisition significantly reduces time, but it often diminishes geometric quality due to lower resolution and exacerbated motion blur, especially in low-light conditions. The main objective of this study is to perform a methodological and feasibility analysis of capturing and photogrammetrically processing videos using 360-degree multi-cameras. We analyse the results across different scenes, focusing on evaluating the accuracy of the outputs. The proposed methodology aims to improve data acquisition efficiency by reducing or eliminating the need for Ground Control Points (GCPs) during the orientation process.

1. Introduction

Heritage documentation primarily relies on geomatic techniques such as Light Detection and Ranging (LiDAR) and photogrammetry. Numerous applications demonstrate the effective use of these techniques, both independently and in combination. For Egyptian hypogea, both approaches are viable. However, while one technique may be adequate for simple scenes, a combination is recommended for complex ones to ensure comprehensive coverage and a certain level of quality. In this context, Pérez-García et al. (2024) define complex scenes as those whose geometric characteristics, location, and accessibility make simple data acquisition difficult or impossible (e.g., narrow spaces with limited sensor-to-object distance). These situations require employing more than one geomatic technique to fully obtain geometry and texture for 3D modelling. This approach aligns with suggestions from several authors (Kadobayashi et al., 2004; Guarnieri et al., 2006; Lerma et al., 2010; Hassan and Fritsch, 2019; Alshawabkeh et al., 2021), who highlight the benefits of leveraging various techniques for complete and accurate products. Furthermore, documenting these scenes demands high acquisition efficiency, often due to limited survey time and the simultaneous execution of other tasks like archaeological work. Data capture frequently requires pausing other activities, leading to delays and increased costs. Consequently, for complex scenes, data acquisition is a critical consideration because achieving complete coverage often requires a large number of photographs (for pinhole cameras and close-range photogrammetry, CRP) or scanning stations (for terrestrial laser scanning, TLS).

In the context of photogrammetry (CRP), various approaches have emerged to cover scenes with fewer images by utilizing lenses that provide a larger Field of View (FoV). These include wide-angle lenses (Martínez et al., 2013; Fiorillo et al., 2016), fisheye lenses (Boulianne et al., 1997; Kedzierski and Fryskowska, 2009; Mandelli et al., 2017; León-Vega and Rodríguez-Laitón, 2019; Perfetti et al. 2019), and 360-degree cameras (Barazzetti et al, 2018; Fangi et al., 2018; Pérez-García et al., 2024), with the latter being considered in this study. This development has led to significant advancements in spherical photogrammetry (Fangi, 2007), which leverages both fisheye images (FEI) and spherical images (SI), also known as panoramic images (Fangi, 2007; Fangi and Nardinocchi, 2013; Jiang et al. 2023). The creation of SI from multiple images (e.g., FEI) typically involves stitching algorithms (Wei et al., 2019; Wang and Yang, 2020; Abbadi et al., 2021). Both FEI and SI can be employed in heritage documentation, each offering advantages and disadvantages that guide their selection based on the specific scene to be surveyed (Pérez-García et al., 2024).

360-degree cameras are classified into three types: diaptic, catadioptic, and polydioptic (Scaramuzza, 2014; Herban et al., 2022; Jiang et al. 2023). In heritage documentation, polydioptic cameras are the most common; these are known as 360-degree multi-cameras and contain multiple fisheye lenses (a minimum of two) to capture scenes with a 360-degree horizontal FoV. When incorporating multiple lenses, these systems achieve high overlaps between adjacent images, which facilitates and improves stitching procedures to obtain SI by using central zones where lens distortion is typically lower. Furthermore, the overlapping of FEI allows for the extraction of other valuable information, such as depth maps, because each point of the scene is captured from multiple viewpoints. Another advantage of FEI over SI is the potential to use extrinsic calibration parameters to establish constraints that simplify the orientation procedure (Perfetti et al., 2018; Huang et al., 2022; Bruno et al., 2024) and minimize the need for Ground Control Points (GCPs) (Pérez-García et al., 2024). Conversely, using SI significantly reduces the number of images processed compared to FEI, specifically by the factor of the number of camera sensors (e.g., a multi-camera with six sensors yields six FEI per capture, but only one stitched SI).

Current advancements in 360-degree cameras enable their use in heritage documentation by improving data acquisition efficiency through expanded sensor coverage (FoV). However, this technology exhibits limitations in geometric accuracy compared to other techniques such as TLS or CRP. To date, spherical photogrammetry has yielded accuracies of various centimetres in various studies (Barazzetti et al., 2017; Sun and Zang, 2019; Herban et al., 2022). Moreover, indoor

environments present additional challenges due to lighting conditions. These advantages and disadvantages become more pronounced when using videos instead of images (videogrammetry), whether through frame selection (Alsadik et al., 2015; Sun and Zhang, 2019) or the integration of video streams into Mobile Mapping Systems (MMS) (Debeunne and Vivet, 2020). While videogrammetry significantly reduces acquisition time, geometric quality often diminishes, primarily due to lower video resolution and issues like motion blur, which are exacerbated in low-light conditions (Alsadik et al., 2015; Sun and Zhang, 2019). The recent increase in the use of 360-degree multi-cameras stems from their inclusion in MMS based on visual-simultaneous localization and mapping (visual-SLAM) (Shi et al., 2012; Debeunne and Vivet, 2020; Ji et al., 2020; Zhang et al., 2021). Building on the work of Pérez-García et al. (2024), this study analyses the implementation of videogrammetry using a 360-degree multi-camera in complex scenes.

1.1 The Necropolis of Qubbet el-Hawa

The necropolis is located on the west bank of the Nile River, near the city of Aswan (Egypt) (Figure 1a). The site comprises over one hundred rock-cut structures (hypogea) dating from various periods of ancient Egypt, although the main tombs are from the Old Kingdom and the Middle Kingdom. These burial areas served as resting places for governors of Elephantine, the southern region of Ancient Egypt, along with their relatives and households (Jiménez-Serrano, 2023). Within this necropolis (Figure 1b), the hypogea exhibit diverse structures depending on their construction period. Broadly, they can be categorized into basic structures (Figure 1c), which consist of a vertical shaft and/or a burial niche, and complex structures, composed of multiple spaces that can reach significant dimensions (e.g., QH31 extends over 30 meters in length). These complex tombs are further divided into public and private (burial) areas. For Middle Kingdom structures, public areas commonly include a hall of pillars (Figure 1d), a corridor, an offering chamber, and a sanctuary or offering chapel. Conversely, the private area features multiple corridors, vertical shafts (up to 14 meters in QH33), burial chambers, and niches. These complex structures present a significant challenge to document graphically due to the presence of narrow and confined spaces, as well as vertical shafts. Additional issues include poor illumination within the tombs and the presence of concurrent archaeological and tourist activities. Consequently, data acquisition tasks often necessitate pausing other ongoing activities. Given these difficulties, acquisition time is a critical factor at such sites, making it essential to employ geomatic techniques that are as efficient as possible while still ensuring the geometric and radiometric quality required by the documentation project. In this context, the use of 360-degree cameras is a feasible option for improving acquisition efficiency in complex scenes.

1.2 Objectives

The main objective of this study is to conduct a methodological and feasibility analysis of capturing and photogrammetrically processing videos using 360-degree multi-cameras in complex heritage scenes. This analysis will be performed both indoors and outdoors, utilizing three scenes from the Necropolis of Qubbet el-Hawa (Aswan, Egypt) that encompass diverse challenges, including sloped and sand-covered areas, simple and narrow niches, and complex structures characterized by narrow spaces, occlusions, and poor illumination conditions. As an additional goal, we also analyse the increase in acquisition efficiency, a fundamental aspect in scenes where other tasks (archaeological, tourist) are commonly present.

This document is structured as follows: First, the implemented methodology and its application to three scenes at this site are described. Second, the primary results obtained are presented, and the advantages and disadvantages of this approach are discussed. Finally, the conclusions and future lines of this study are proposed.

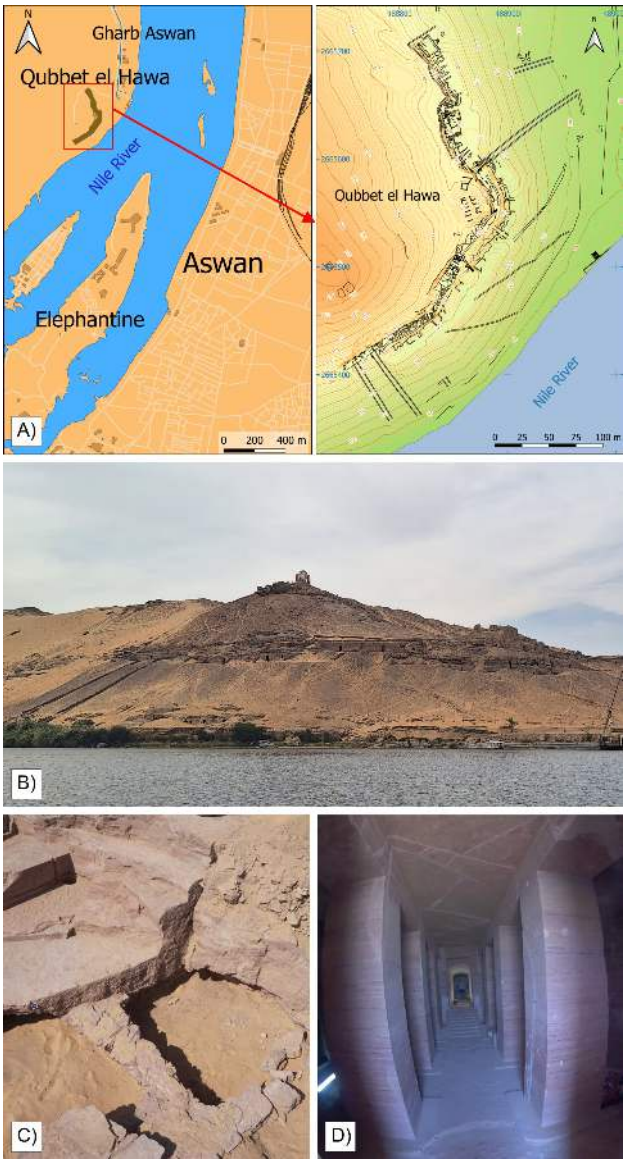

Figure 1. Necropolis of Qubbet el-Hawa: a) Location; b) general view of the hill; c) archaeological survey in QH34 area; d) hall of pillars of QH31.

2. Methodology and application

The methodology proposed in this study (Figure 2) evaluates the accuracy of documentation results with the aim of improving data acquisition efficiency by reducing or eliminating the need for GCPs during the orientation and georeferencing processes.

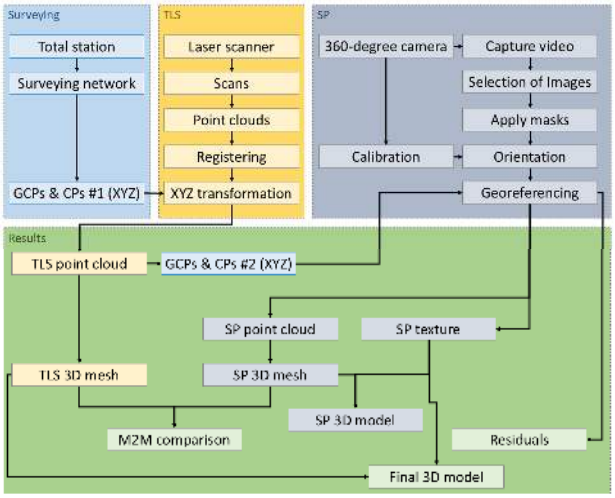

Figure 2. Methodology developed in this study.

The workflow is divided into four sections: surveying, TLS, SP and results analysis:

1. Surveying is conducted to obtain sets of GCPs and Checkpoints (CPs), which are used to georeference and check products from the other techniques. For this purpose, a total station is employed to establish a surveying network for each study area (e.g., a burial structure). This network of topographic points extends from a main network covering the entire site. From these points, the coordinates of a set of well-distributed targets across the scene are obtained (GCPs & CPs #1 in Figure 2).

2. TLS data is acquired using a laser scanner, distributing multiple scans to obtain dense point clouds without colour registration. The location and number of scan stations are determined by the scene’s characteristics and structure, ensuring complete coverage and significant overlap between adjacent scans to facilitate relative point cloud registration. Once all point clouds are registered, a rigid 3D transformation is applied to generate the final TLS point cloud. From this product, coordinates of additional GCPs and CPs (GCPs & CPs #2 in Figure 2) are also extracted; these are used to georeference SP products.

3. SP is developed using a 360-degree multi-camera with pre-calibrated intrinsic and extrinsic parameters (distances between the sensors). Subsequently, video capture is carried out following a scheme designed for data completeness and to minimize drift issues during the photogrammetric orientation of the data. To achieve this, captures are performed by creating loops, ensuring the most complete matching graph possible. The next step involves extracting frames from the video to obtain a set of Fisheye Images (FEI). During this process, the minimum frames per second (fps) are selected, and a sharpness analysis is performed on the images to identify the sharpest frames within the chosen interval. Blur detection techniques, widely described by Pertuz et al. (2013) and Pagaduan et al. (2020), were applied using an approach based on the Fast Fourier Transform in the frequency space. Once the images are selected, and particularly for interior cases, a contrast enhancement method based on an improved adaptive gamma correction, as proposed by Cao et al. (2018), is applied to improve their radiometric quality. After that, masks are applied to remove areas of FEI that contain objects unrelated to the scene, such as the operator, mast, or illumination system (in interior cases), as well as burned areas. Following this, the photogrammetric orientation process is conducted without the use of GCPs. The software Metashape, along with its Python API, is used to implement a script that incorporates the distances between sensors via the scale option. After this process, the georeferencing of the photogrammetric products is performed with a rigid 3D transformation, considering a reduced set of well-distributed GCPs (e.g., four GCPs) because the scale of the photogrammetric block is already defined by the distances between sensors.

4. For results, a 3D model of the scene is generated, with geometry based on the SP point cloud and texture extracted from SP images. Furthermore, residuals resulting from the 3D transformation (using a minimum number of GCPs) applied to the SP products are obtained. Also, residuals from the georeferencing developed using a traditional GCP-based procedure, obtained using CPs, are calculated. Distances between 3D meshes (TLS vs. 360-degree video) are also analysed by performing a mesh-to-mesh (M2M) comparison (M2M in Figure 2). This data allows for a statistical analysis of all residuals obtained from georeferencing and distances between 3D meshes. The final 3D model is obtained using the TLS 3D mesh and SP texture.

Figure 3. 360-degree camera used in this study: a) view of the camera; b) schema of FoV and overlap; c) video acquisition in the QH525 area; d) video acquisition in QH31.

The methodology was applied to three scenes within the Necropolis of Qubbet el-Hawa, each presenting distinct characteristics that pose challenges for photogrammetric and TLS techniques, particularly concerning data capture. Specifically, an external area, a combination of external and internal zones, and an internal burial structure were selected for this application.

- Scene 1: QH525 area. Located on a hillside with slopes of approximately 30 meters and an incline greater than 50%. This zone is covered in sand, though some rocks and structures are visible. Both the slope and the sand complicated data acquisition.
- Scene 2: QH34gg tomb and adjacent area. This scene consists of small niches open to the outside (Figure

1c). It was considered complex due to the reduced dimensions of these niches.

- Scene 3: QH31 tomb. This focuses on the public area, which integrates a hall of pillars (Figure 1d), a corridor, an offering chamber, and the sanctuary, extending approximately 30 meters into the rock. It was also deemed complex due to occlusions caused by its structure (e.g., pillars), the presence of narrow spaces (e.g., corridor), poor illumination conditions, and the need for rapid acquisition due to tourist presence.

	QH525	QH34gg	QH31
Exterior/Interior	E	E/I	I
Area (m²)	4000	190	142
Number of scans	11	13	15
Video duration (mm:ss)	19:20	4:05	3:00
Number of images (x6)	1160	245	180

Table 1. Summary of the application carried out in this study

In the application of the methodology, surveying tasks were performed using a Leica TCR403 total station, and TLS was conducted with a Faro Focus X130 scanner. For TLS, scanning was configured with a density of approximately 7 millimetres at 10 meters, and registration was performed without colour. With this configuration, each scan station required less than 6 minutes. SP was developed using an Obsidian Kandao Go camera (Figure 3a). This camera incorporates six fisheye lenses, each with a FoV of 220 degrees (Figure 3b), allowing for video capture at a resolution of 1728x1728 and 30 fps. In exterior cases, the camera was mounted on a mast up to 2 meters high to ensure full scene coverage and avoid occlusions (Figure 3c). In the interior scene, the camera was placed on a mast of 1 meter with an auxiliary illumination system consisting of an LED lamp attached to the upper part of the camera and powered by a portable battery (Figure 3d). The location of this system was chosen to minimize its appearance in the FEI images, although these areas were subsequently excluded using masks. The light intensity was regulated considering the average distance from the object to prevent over or poorly illuminated areas. Table 1 summarizes the main features of the application carried out in this study by areas. In addition, Figure 4 shows an example of the pre-processing of the extracted images (Figure 4a), including a contrast enhancement (Figure 4b) and masking (Figure 4c).

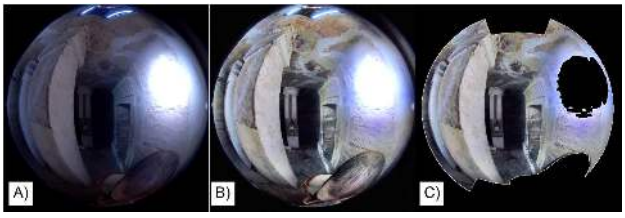

Figure 4. Example of pre-processing images: a) frame selection; b) contrast enhancement; c) masking.

Figure 5 shows a scheme of image locations after the orientation procedure. Figure 5a depicts the overall trajectory followed by the operator during data acquisition. In this scheme, scale bars defined between the six images obtained at each frame selection time are included. These scale bars were derived from the extrinsic calibration parameters. Figure 5b provides a detailed view of how six images are oriented at a certain time, further illustrating these scale bars.

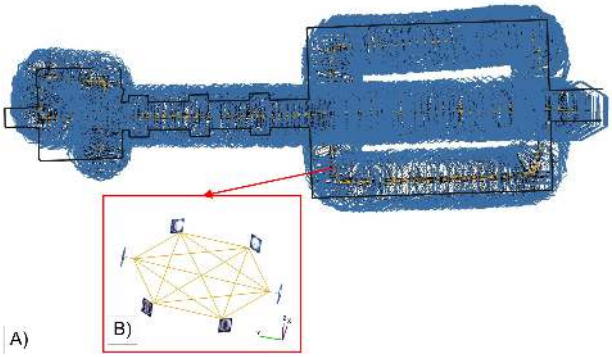

Figure 5. Scheme of oriented images in QH31: a) extracted images showing the trajectory followed by the operator; b) detailed view of six images oriented at a certain time.

3. Results and discussion

The results of this study are evaluated by contrasting the 3D models obtained in each area. Positional accuracy is analysed through the residuals of the 3D transformation and the distances between SP and TLS meshes. Texture quality is checked visually, considering the requirements of the project.

3.1 3D models

Figure 6 displays the textured 3D models for all three scenes resulting from the proposed methodology, utilizing SP for both geometry and texture. The QH525 (Figure 6a) and QH34gg (Figure 6b and Figure 6c) models exhibited satisfactory quality for both texture and 3D reconstruction, meeting the specified resolution requirements. Conversely, the QH31 model (Figure 6d and Figure 6e) showed poorer quality, primarily due to noise in the 3D mesh (Figure 6f), particularly in darker areas such as ceilings and floors. In terms of texture quality, there were some issues with specific areas containing painted decoration, where the resolution was poor (Figure 6g).

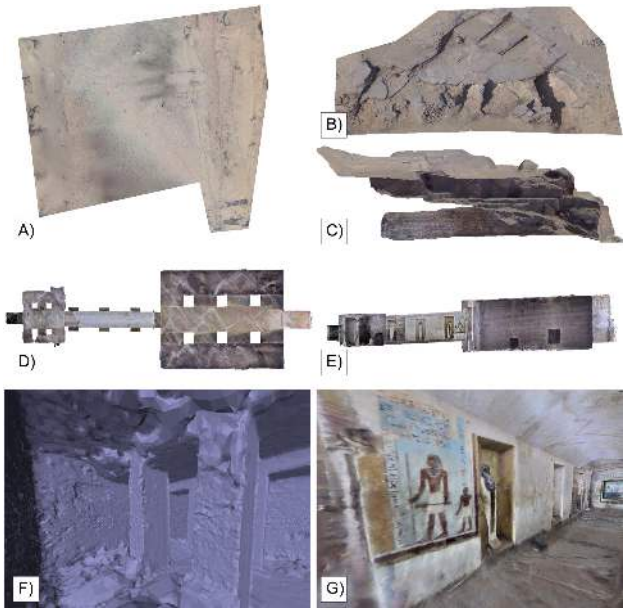

Figure 6. Views of the 3D models: a) top view of QH525; b) top view of QH34gg; c) lateral view of QH34gg; d) top view of QH31; e) lateral view of QH31; f) detailed view of 3D mesh

(offering chamber of QH31); g) detailed view of the 3D model (corridor of QH31) including some painted areas.

3.2 3D transformation and M2M comparison

The residuals of the CPs are calculated following the determination of the 3D transformation parameters. For each scene, four GCPs were selected to define these parameters. These points were intentionally located in areas separate from the CPs to avoid influencing their residuals and to effectively study drift issues. Therefore, the GCPs were positioned in the initial areas of the trajectory, while CPs were placed in the final zones. For instance, in QH31, GCPs were chosen within the hall of pillars, while the CPs were located in the offering chamber.

The statistics of these georeferencing residuals (mean, standard deviation, minimum, and maximum) are presented in Figure 7a. The maximum residual values for QH525 and QH34gg are 4.8 centimetres and 6.9 centimetres, respectively, while for QH31, this value exceeds 10 centimetres. These maximum values occur in the offering chamber at the end of the corridor.

To ensure global quality control of the products, a surface comparison is conducted between the TLS and SP data. Figure 7b presents the distance histogram and the corresponding statistics table, comparing the surfaces of all three scenes. This analysis reveals a similar trend to the point-based analysis, with QH31 exhibiting the poorest results, showing an average distance of 2.4 centimetres and a standard deviation of 7.7 centimetres.

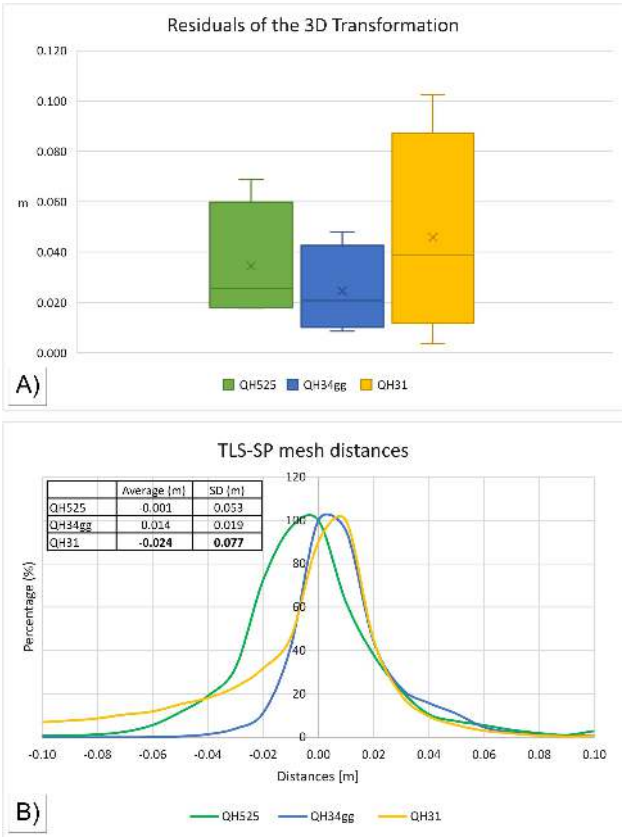

Figure 7. Results: a) residuals of the 3D transformation; b) TLS-SP M2M distances.

Furthermore, Figure 8 displays the coloured surfaces of the three scenes, rendered with a distance-based colour palette. Figures 8d and Figure 8e show the results for QH31, where the previously mentioned errors are more clearly visible. These views highlight errors in the floor and ceiling areas of the hall of pillars. This space comprises three naves; the central nave benefits from ambient light due to its direct access to the tomb entrance. In this central nave, and on the edges of the pillars oriented towards it, the differences between the models are within the range of 2 centimetres. However, the two lateral naves lack ambient light, and errors attributable to this condition are observable. On the other hand, drift errors during the orientation process are clearly visible, progressively increasing along the corridor and the offering chamber, where these differences are on the order of 10 centimetres. Specifically, this drift is predominantly observed in the XY plane, causing a certain turn. In the QH34gg and QH525 scenes, the highest differences primarily occur in areas with occlusions or edge effects, attributable to variations in resolution and model smoothing. However, these affected areas are insignificant compared to the total surface area.

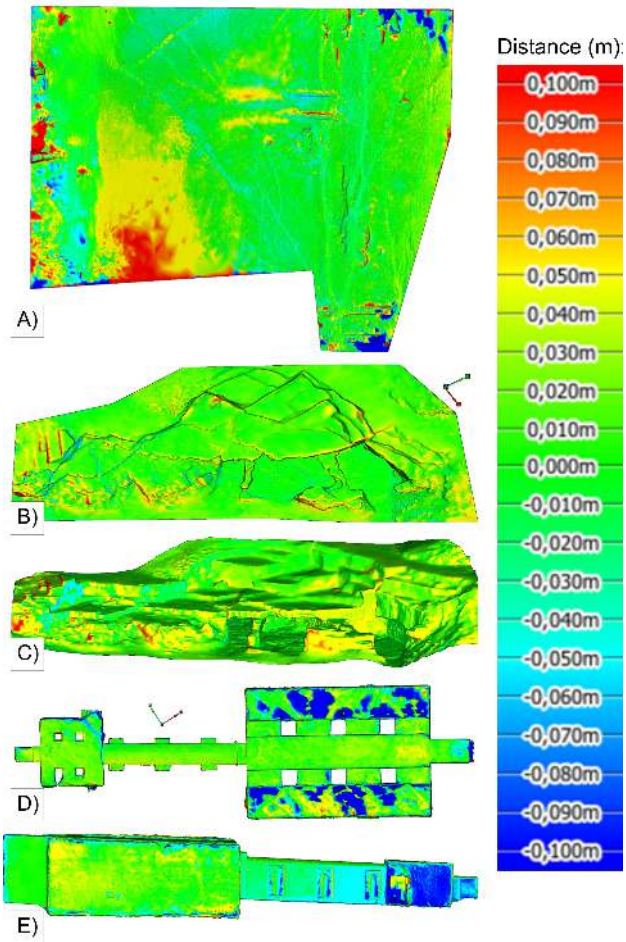

Figure 8. Views of 3D models coloured with M2M distances.

3.3 Discussion

The analysis of the products obtained in this study suggests a good performance in both geometry and texture when using SP videogrammetry in external areas. Conversely, internal areas have shown some issues related to illumination conditions in poorly-lighted scenes, affecting both attributes. In these scenes, distances from the light source to the object are sometimes highly variable across 360 degrees, which can lead to zones that are either over or poorly exposed to artificial light. In these cases, using the TLS point cloud to define the geometry is a necessary alternative, while the texture is generally adequate for

non-decorated areas, considering project requirements. These areas specifically demand higher resolution—for example, by using still images from conventional cameras or SP, and by adding improved illumination systems. Despite these issues, the approach described in this study demonstrates significant improvement in acquisition efficiency, which is fundamental for this type of project.

4. Conclusions

This study builds upon the work of Pérez-García et al. (2024), who analysed the advantages of using 360-degree multi-cameras and demonstrated their efficiency in complex heritage scenes. While their analysis focused on still images, our work extends this by examining the capture and processing of videos across three distinct, challenging scenes to determine the technique's applicability in such environments.

Data acquisition enables massive capture (30 fps), allowing for the selection of the most suitable images based on geometric and radiometric quality. However, although video capture improves acquisition efficiency, 360-degree camera videos typically exhibit lower resolution and a higher susceptibility to motion blur. Nonetheless, the geometric errors obtained indicate that these image types are suitable for most heritage documentation studies, particularly in well-lit conditions. The primary limitation arises from image sharpness in darker areas. For indoor environments with restricted distances and dimensions (e.g., niches or vertical shafts), this technique offers a compelling alternative to methods like TLS or CRP, significantly reducing acquisition times.

Regarding the orientation process, this study opted against using control points during the initial photogrammetric processing. Instead, a minimal number of points were used solely for georeferencing via a 3D transformation, confirming previous studies. The results obtained are directly tied to these conditions, where image quality significantly influences processing. However, the object's geometry can also play a significant role, as an unsuitable capture scheme can prevent the successful implementation of the loop strategy, which is fundamental for obtaining reliable products. For example, this is evident in the QH31 corridor area, where drift issues are increased.

Future work will involve implementing the methodology in additional scenes, improving both the lighting system and camera quality, and utilizing deep learning methods to enhance blurred images. Furthermore, the integration of low-cost LiDAR systems with SLAM techniques will be explored to further improve the obtained results.

Acknowledgements

The authors would like to thank the support of the Qubbet el-Hawa Research Project, developed during the last 17 years by the University of Jaén (Spain).

References

Abbadi, N.K.E., Al Hassani, S.A., Abdulkhaleq, A.H., 2021. A review over panoramic image stitching techniques. *J. Phys. Conf. Ser.*, 1999, 012115. doi.org/10.1088/1742-6596/1999/1/012115

Alsadik, B., Gerke, M., Vosselman, G., 2015. Efficient use of video for 3D modelling of cultural heritage objects. *ISPRS Ann. Photogramm. Remote Sens. Spat. Inf. Sci.*, II-3/W4, 1-8. doi.org/10.5194/isprsannals-II-3-W4-1-2015

Alshawabkeh, Y., Baik, A., Miky, Y., 2021. Integration of laser scanner and photogrammetry for heritage BIM enhancement. *ISPRS Int. J. Geo-Inf.*, 10(5), 316. doi.org/10.3390/ijgi10050316

Barazzetti, L., Previtali, M., Roncoroni, F., 2017. Fisheye lenses for 3D modeling: evaluations and considerations. *Int. Arch. Photogramm. Remote Sens. Spatial Inf. Sci.*, XLII-2/W3, 79-84. doi.org/10.5194/isprs-archives-XLII-2-W3-79-2017

Barazzetti, L., Previtali, M., Roncoroni, F., 2018 Can we use low-cost 360 degree cameras to create accurate 3D models? *Int. Arch. Photogramm. Remote Sens. Spatial Inf. Sci.*, XLII-2, 69-75. doi.org/10.5194/isprs-archives-XLII-2-69-2018

Boulianne, M., Nolette, C., Agnard, J.P., Brindamour, M., 1997. Hemispherical photographs used for mapping confined spaces. *Photogramm. Eng. Remote Sens.*, 63, 1103-1108.

Bruno, N., Perfetti, L., Fassi, F., Roncella, R., 2024. Photogrammetric survey of narrow spaces in cultural heritage: Comparison of two multi-camera approaches. *Int. Arch. Photogramm. Remote Sens. Spatial Inf. Sci.*, 48, 87-94. doi.org/10.5194/isprs-archives-XLVIII-2-W4-2024-87-2024

Cao, G., Huang, L., Tian, H., Huang, X., Wang, Y., Zhi, R., 2018. Contrast enhancement of brightness-distorted images by improved adaptive gamma correction. *Comput. Electr. Eng.*, 66, 569-582. doi.org/10.1016/j.compeleceng.2017.09.012

Debeunne, C., Vivet, D., 2020. A review of visual-LiDAR fusion based simultaneous localization and mapping. *Sensors*, 20(7), 2068. doi.org/10.3390/s20072068

Fangi, G., 2007. The multi-image spherical panoramas as a tool for architectural survey. *Int. Arch. Photogramm. Remote Sens. Spatial Inf. Sci.*, 36(5/C53), 311-316.

Fangi, G., Nardinocchi, C., 2013. Photogrammetric Processing of Spherical Panoramas. *Photogramm. Rec.*,28, 293-311. doi.org/10.1111/phor.12031

Fangi, G., Pierdicca, R., Sturari, M., Malinverni, E.S., 2018 Improving spherical photogrammetry using 360° omni-cameras: Use cases and new applications. *Int. Arch. Photogramm. Remote Sens. Spatial Inf. Sci.*, XLII-2, 331-337. doi.org/10.5194/isprs-archives-XLII-2-331-2018

Fiorillo, F., Limongiello, M., Fernández-Palacios, B.J., 2016. Testing GoPro for 3D model reconstruction in narrow spaces. *Acta IMEKO* 2016, 5, 64-70. orcid.org/0000-0001-6755-7928

Guarnieri, A., Remondino, F., Vettore, A., 2006. Digital photogrammetry and TLS data fusion applied to Cultural Heritage 3D modeling. *Int. Arch. Photogramm. Remote Sens. Spatial Inf. Sci.*, XXXVI (Part 5).

Hassan, A.T., Fritsch, D., 2019. Integration of laser scanning and photogrammetry in 3D/4D cultural heritage preservation–a review. *International Journal of Applied Science and Technology*, 9(4), 16. doi.org/10.30845/ijast.v9n4p9

Herban, S., Costantino, D., Alfio, V.S., Pepe, M., 2022 Use of low-cost spherical cameras for the digitisation of cultural

heritage structures into 3D point clouds. *J. Imaging*, 8, 13. doi.org/10.3390/jimaging8010013

Huang, D., Elhashash, M., Qin, R., 2022. Constrained bundle adjustment for structure from motion using uncalibrated multi-camera systems. *ISPRS Ann. Photogramm. Remote Sens. Spat. Inf. Sci.*, V-2-2022, 17-22. doi.org/10.5194/isprs-annals-V-2-2022-17-2022

Ji, S., Qin, Z., Shan, J., Lu, M., 2020. Panoramic SLAM from a multiple fisheye camera rig. *ISPRS J. Photogramm. Remote Sens.*, 159, 169-183. doi.org/10.1016/j.isprsjprs.2019.11.014

Jiang, S., Li, Y., Weng, D., You, K., Chen, W., 2023. 3D reconstruction of spherical images: A review of techniques, applications, and prospects. Geo-Spat. Inf. Sci., 27(6), 1959-1988. doi.org/10.1080/10095020.2024.2313328

Jiménez-Serrano, A. 2023. *Descendants of a Lesser God: Regional Power in Old and Middle Kingdom Egypt*. American University in Cairo Press, Cairo, Egypt. doi.org/10.2307/jj.809346

Kadobayashi, R., Kochi, N., Otani, H., Furukawa, R., 2004. Comparison and evaluation of laser scanning and photogrammetry and their combined use for digital recording of cultural heritage. *Int. Arch. Photogramm. Remote Sens. Spatial Inf. Sci.*, 35(5), 401-406.

Kedzierski, M., Fryskowska, A., 2009. Application of digital camera with fisheye lens in close range photogrammetry. *Proceedings of the ASPRS 2009 Annual Conference*, Baltimore, USA, 9-13.

León-Vega, H.A., Rodríguez-Laitón, M.I., 2019. Fisheye Lens Image Capture Analysis for Indoor 3d Reconstruction and Evaluation. *Int. Arch. Photogramm. Remote Sens. Spatial Inf. Sci.*, XLII-2/W17, 179-186. doi.org/10.5194/isprs-archives-XLII-2-W17-179-2019

Lerma, J.L., Navarro, S., Cabrelles, M., Villaverde, V., 2010. Terrestrial laser scanning and close range photogrammetry for 3D archaeological documentation: the Upper Palaeolithic Cave of Parpalló as a case study. *J. Archaeol. Sci.* 37(3), 499-507. doi.org/10.1016/j.jas.2009.10.011

Mandelli, A., Fassi, F., Perfetti, L., Polari, C. 2017. Testing different survey techniques to model architectonic narrow spaces. *Int. Arch. Photogramm. Remote Sens. Spatial Inf. Sci.*, XLII-2/W5, 505-511. doi.org/10.5194/isprs-archives-XLII-2-W5-505-2017

Martínez, S., Ortiz, J., Gil, M.L., Rego, M.T., 2013. Recording complex structures using close range photogrammetry: The cathedral of Santiago de Compostela. *Photogramm. Rec.*, 28(144), 375-395. doi.org/10.1111/phor.12040

Pagaduan, R.A., Aragon, R., Medina, R.P., 2020. iBlurDetect: Image blur detection techniques assessment and evaluation study. In *International Conference on Culture Heritage, Education, Sustainable Tourism, and Innovation Technologies (CESIT2020)*, 286-291. doi.org/10.5220/0010307700003051

Pérez-García, J.L., Gómez-López, J.M., Mozas-Calvache, A.T., Delgado-García, J., 2024. Analysis of the Photogrammetric Use of 360-Degree Cameras in Complex Heritage-Related Scenes: Case of the Necropolis of Qubbet el-Hawa (Aswan Egypt). *Sensors*, 24(7), 2268. doi.org/10.3390/s24072268

Pertuz, S., Puig, D., Garcia, M.A., 2013. Analysis of focus measure operators for shape-from-focus. *Pattern Recognit.*, 46(5), 1415-1432. doi.org/10.1016/j.patcog.2012.11.011

Perfetti, L., Polari, C., Fassi, F., 2018. Fisheye Multi-Camera System Calibration for Surveying Narrow and Complex Architectures. *Int. Arch. Photogramm. Remote Sens. Spatial Inf. Sci.*, XLII-2, 877–883. doi.org/10.5194/isprs-archives-XLII-2-877-2018

Perfetti, L., Fassi, F., Rossi, C., 2019. Fisheye Photogrammetry to Generate Low–Cost DTMs. *Int. Arch. Photogramm. Remote Sens. Spatial Inf. Sci.*, XLII-2/W17, 257-263. doi.org/10.5194/isprs-archives-XLII-2-W17-257-2019

Scaramuzza, D., 2014. Omnidirectional camera. In Computer Vision, Springer, Boston, USA, pp. 552-560. doi.org/10.1007/978-0-387-31439-6_488

Shi, Y., Ji, S., Shi, Z., Duan, Y., Shibasaki, R., 2012. GPS-supported visual SLAM with a rigorous sensor model for a panoramic camera in outdoor environments. *Sensors*, 13, 119-136. doi.org/10.3390/s130100119

Wei, L.Y.U., Zhong, Z., Lang, C., Yi, Z.H.O.U., 2019. A survey on image and video stitching. *Virtual Real. Intell. Hardw.*, 1, 55-83. doi.org/10.3724/SP.J.2096-5796.2018.0008

Wang, Z., Yang, Z., 2020. Review on image-stitching techniques. *Multimed. Syst.*, 26, 413-430. doi.org/10.1007/s00530-020-00651-y

Zhang, Y., Huang, F., 2021. Panoramic visual slam technology for spherical images. *Sensors* 2021, 21, 705. doi.org/10.3390/s21030705